Effect of Cross-Link Density on the Internal Structure of Poly(N-isopropylacrylamide) Microgels

ARTICLE *in* THE JOURNAL OF PHYSICAL CHEMISTRY B · AUGUST 2001

Impact Factor: 3.3 · DOI: 10.1021/jp004600w

5 AUTHORS, INCLUDING:

Imre Varga
Eötvös Loránd University
65 PUBLICATIONS **1,437** CITATIONS
SEE PROFILE

Tibor Gilányi
KTH Royal Institute of Technology
68 PUBLICATIONS **1,200** CITATIONS
SEE PROFILE

Róbert Mészáros
Eötvös Loránd University
59 PUBLICATIONS **1,276** CITATIONS
SEE PROFILE

Miklos Zrinyi
Semmelweis University
149 PUBLICATIONS **3,101** CITATIONS
SEE PROFILE

Effect of Cross-Link Density on the Internal Structure of Poly(*N*-isopropylacrylamide) Microgels

Imre Varga,*,† Tibor Gilányi,† Róbert Mészáros,† Genoveva Filipcsei,‡ and Miklós Zrínyi‡

Department of Colloid Chemistry, Loránd Eötvös University, P.O. Box 32, H-1518 Budapest 112, Hungary, and Department of Physical Chemistry, Technical University of Budapest, H-1521 Budapest, Hungary

Received: December 31, 2000; In Final Form: May 8, 2001

The effect of cross-link density on the structure of Poly-(N-isopropylacrylamide) microgel particles prepared by emulsion polymerization was investigated by static and dynamic light scattering measurements. According to these measurements the gel particles cannot be considered as homogeneous spheres. The structure of the gel particles strongly depends on the degree of cross-linking. At high cross-link density the particles can be described with a Gaussian segment density distribution. With decreasing cross-link density the structure of the microgel particles tends toward that of a highly branched coil.

Introduction

Stimuli-responsive hydrogels have attracted a widespread interest in the past decade. These materials can change their swelling and shrinking in response to environmental changes.[1,2] The stimuli that have been investigated to induce changes in polymer gels are diverse, and they include temperature, pH, solvent and ionic composition, electric field, light intensity, and an introduction of specific molecules. The applications of these gels can be utilized e.g. in mechanical devices and separation systems.[3]

The disadvantage of macroscopic hydrogels is their slow response to the changes in the external conditions. However, this problem can be overcome by the preparation of microgels. Microgel particles are cross-linked macromolecules that swell in the solvent. They have several orders of magnitudes smaller characteristic dimensions (10 nm−1 μm) than that of the macrogels resulting in a considerably accelerated kinetic behavior. Besides their technical applications (e.g. surface coatings, rheological control and stabilizing agents[4−6]) microgels are promising candidates for the development of biochemical and biomedical applications, controlled drug delivery systems, and heavy metal scavengers.[7,8] Furthermore, they have also been considered as model systems to investigate order−disorder and glass transitions[9,10] and polymer chain dynamics.[11]

Poly(N-isopropylacrylamide) hydrogel, abbreviated as PNIPAM gel, is one of the most frequently studied temperature-responsive hydrogels. PNIPAM gels exhibit a remarkable shrinking with increasing temperature and they exhibit a volume-phase transition around 33 °C.[12] This volume-phase transition has been intensively studied in case of macro and microgels as well as for linear PNIPAM polymers.[13−17]

In the case of PNIPAM microgels, the majority of the experimental work has focused on the factors governing the swelling and de-swelling behavior of the microgel particles.[18−24] Though the structure of microgel particles plays an important role in the determination of the swelling properties, the question of inner-particle structure has not been addressed yet. However, there are a few indications in the literature that the microgel particles possess an inhomogeneous inner structure. Kinetic measurements showed that the cross-linking monomer has a higher polymerization rate than the PNIPAM monomer suggesting radially decreasing cross-link density in the particles.[25,26] The investigation of the static structure factor of concentrated polystyrene microgels indicated soft interaction potentials, which were attributed to the dangling polymer ends at the surface of the particles.[27] Rheological studies of concentrated microgel dispersions also indicated soft interaction potentials between the particles.[28,29] Recently, we found significant deviation from the form factor of a spherical particle with constant segment density by static light-scattering measurements in case of a strongly cross-linked PNIPAM microgel.[30]

The aim of this work was the characterization of the internal structure of the PNIPAM microgel particles in their swollen state and a systematic investigation of the effect of the average cross-link density on this structure.

Experimental Section

Preparation of PNIPAM Microgel Latex. For the preparation N-isopropylacrylamide (NIPAM), methylenbisacrylamide (BA), ammonium persulfate (APS), and sodium dodecyl sulfate (SDS) were used. These chemicals were provided by Aldrich and were used for the preparation without further purification. Our procedure was based on the method developed by Wu et al.[31] 7.0 g NIPAMM, varying amount of cross-linker BA (0.000−0.700 g) and 94 mg SDS were dissolved in 470 mL distilled water. The temperature of the reactor was kept at 60 °C and the solution was intensively stirred. To remove oxygen, nitrogen gas was purged through the solution for 30 min. Then, 0.14 g APS dissolved in 30 mL water was mixed with the solution and it was followed by intensive stirring for 4 h. The PNIPAM latex was purified from unreacted monomers and surfactant by dialysis against distilled water for 4 weeks. To ensure the complete removal of the ionic surfactant from the samples used for light scattering measurements, they were further purified by mixed-bed cation/anion exchange. This method was originally developed for the elimination of ionic contaminants in case of latex dispersion.[32]

* To whom correspondence should be addressed. E-mail: imo@para.chem.elte.hu. Fax.: 209-0602.

† Loránd Eötvös University.

‡ Technical University of Budapest.

10.1021/jp004600w CCC: $20.00
Published on Web 08/24/2001

Eight PNIPAM samples were prepared with different cross-link densities. For the indication of the average cross-link densities of the samples we used the molar ratio of the NIPAM monomer to the cross-linker BA. Using this notation the average cross-link densities of the prepared samples can be given as follows: N13, N30, N50, N70, N200, N300, N400, polymer (without cross-linker).

Static and Dynamic Light Scattering Measurements. Static and dynamic light scattering measurements were performed by means of dynamic light scattering equipment (Brookhaven) consisting of a BI-200SM goniometer and a BI-9000AT digital correlator. An argon-ion laser (Omnichrome, model 543AP) operating at 488 nm wavelength and emitting vertically polarized light was used as the light source. The signal analyzer was used in real-time "multi tau" mode. In this mode the time axis was logarithmically spaced over an appropriate time interval and the correlator used 218 time channels. The pinhole was 100 μm.

Time-averaged scattered light intensities were measured at scattering angles from 15 to 155° at different microgel concentrations. The reduced scattering intensities R_ϑ were calculated according to the standard procedures using benzene as the reference with known absolute scattering intensity (3.86×10^{-5} cm^{-1}). The volume-corrected scattering intensities of the benzene varied by less than ± 2% in the angular range from 15° to 155°, demonstrating the good calibration of the instrument. Backscattering correction was also applied for the asymmetrically scattering microgel samples.

The microgel samples were cleaned of dust particles by filtering through 0.8-μm pore-size membrane filters (Millipore) in a closed filtration circuit.

Data Analysis. In dynamic light-scattering experiments the intensity−intensity time-correlation function $g_2(q,\tau)$ was measured (homodyne method) which was converted to the normalized electric field autocorrelation function $g_1(q,\tau)$ by means of the Siegert relation:

$$b|g_1(q,\tau)|^2 = (g_2(q,\tau) - A)/A \qquad (1)$$

where A is the experimentally determined baseline, b ($0 < b < 1$) is a constant that depends on the number of coherence areas seen by the detector, and $q = (4\pi n/\lambda_o)\sin(\vartheta/2)$ is the scattering vector in which n is the refractive index of the solution, λ_o is the wavelength of the incident light in a vacuum, and ϑ is the scattering angle. $g_1(q,\tau)$ is related to the distribution of relaxation rates ($G(\Gamma)$) through a Laplace transformation:

$$g_1(q,\tau) = \int_0^\infty G(q,\Gamma)\exp(-\Gamma\tau)\,d\Gamma \qquad (2)$$

where Γ is the relaxation rate. Since the recovery of $G(q,\Gamma)$ from the experimentally determined $g_1(q,\tau)$ is an ill-posed problem, several numerical methods have been developed for the analysis of the measured autocorrelation function. In this work we used the cumulant expansion that gives reliable results in case of narrow distributions of Γ. This method has the advantage of getting $\bar{\Gamma}(q)$ and $\mu_2 = \int(\Gamma - \bar{\Gamma})^2 G(\Gamma)\,d\Gamma$ (the so-called first and second cumulants), without any prior knowledge about $G(q,\Gamma)$.

If the intensity fluctuation of the scattered light is due to the translational motion of the particles, the mutual diffusion coefficient ($D_m(q)$) can be calculated from the mean relaxation rate by the following relation:

$$D_m(q) = \bar{\Gamma}(q)/q^2 = D_0(1 + CR_g^2q^2) \quad (c \to 0) \qquad (3)$$

in which R_g is the radius of gyration and C is a constant. D_o is related to the equivalent hydrodynamic diameter of the particles (d_h) through the Stokes−Einstein relation

$$D_o = \frac{kT}{3\pi\eta d_h} \qquad (4)$$

where k is the Boltzmann constant, T is the temperature, and η is the viscosity of the medium.

The reduced second cumulant $\mu_2/\bar{\Gamma}^2$ can be related to the polydispersity of the samples ($u = M_w/M_n^{-1}$) according to the following equation:[33,34]

$$\frac{\mu_2}{\bar{\Gamma}^2} = u(1 + u) \qquad (5)$$

Static light scattering data are usually analyzed in terms of the classical Zimm equation, yielding the weight averaged molecular weight (M_w), the z-mean of the square of the radius of gyration ($R_{g,z}^2$), and the second virial coefficient (A_2) as the result of the analysis

$$\frac{Kc}{R_\vartheta} = \frac{1}{M_w}\left(1 + \frac{q^2}{3}R_{g,z}^2\right) + 2A_2c \quad (c \to 0,\ \vartheta \to 0) \qquad (6)$$

where $K = [2\pi n_o(dn/dc)]^2 N_A^{-1}\lambda_o^{-4}$, c is the concentration of the particles, dn/dc is the refractive index increment, and N_A is the Avogadro's number.

The angular dependence of the reduced-scattering intensity often contains further information on the particle shape. In general, Kc/R_ϑ can be given in the following form for monodisperse systems:

$$\frac{Kc}{R_\vartheta} = \frac{1}{MP_\upsilon} + 2A_2c \quad (c \to 0) \qquad (7)$$

where P_ϑ is the particle scattering function, which depends on the particle shape.

More detailed discussions on light scattering theory are available in several textbooks.[35−37]

Results and Discussion

For the characterization of the synthesized PNIPAM microgels we performed dynamic light-scattering measurements. The measured autocorrelation functions plotted against $q^2\tau$ were found to be independent of the scattering angle in the case of every cross-link density. The $g_1(\tau)$ functions were also independent of the microgel concentration in the investigated, very dilute concentration range (from 4×10^{-5} to 2×10^{-4} g·cm^{-3}). The cumulant analysis of the autocorrelation functions indicated extremely narrow size distributions of the gel particles. A typical value of the reduced second cumulant was $p = 0.02 \pm 0.01$. This means that the gel particles can be well characterized with a single relaxation time or diffusion coefficient and can be considered practically monodisperse in case of each cross-link density. This is supported by the observation that under appropriate conditions all of the microgel samples formed colloidal crystals.

In Figure 1 the temperature-dependent swelling of some of the prepared PNIPAM microgels is shown. To compare the swelling behavior of the different cross-link density samples, the measured hydrodynamic diameters (d_h) are normalized by their values measured at 40 °C in the collapsed state of the microgels. As can be seen, the critical temperature of the volume-phase transition shows only a slight dependence on the

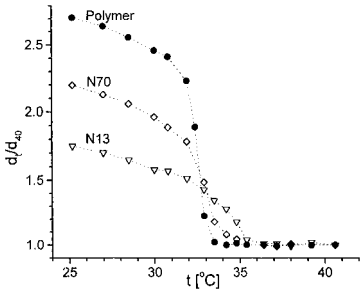

Figure 1. Normalized hydrodynamic diameter of the PNIPAM microgels (N13, N70, and polymer) vs temperature.

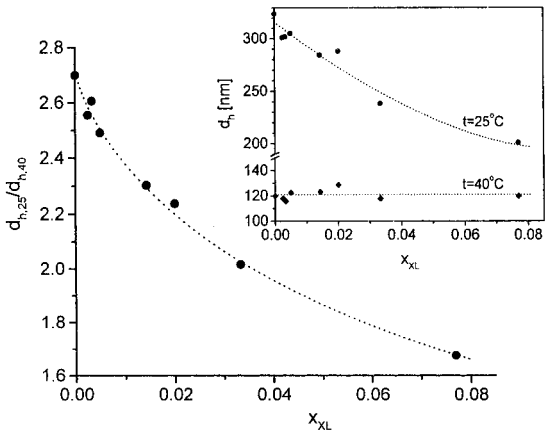

Figure 2. Dependence of the microgel particle swelling on the cross-link density.

cross-link density of the PNIPAM microgels. This observation is in agreement with the investigations of Inomata et al.[38] on PNIPAM macrogels and with the experimental results of Senff et al.[29] on PNIPAM microgels.

Figure 1 also demonstrates that with increasing cross-link density the relative swelling of the microgel particles decreases. This is illustrated in Figure 2, in which the hydrodynamic diameter of the PNIPAM microgels measured at 25 °C and normalized by their values at 40 °C is plotted against the mole fraction of the cross-linker (x_{BA}). The cross-link density of the microgel particles has a strong effect on the swelling. The indicated diameter ratios correspond to a 20-times volume increase in case of the polymer ($x_{BA} = 0$), while "only" a 5-times volume increase was found for the most cross-linked microgel (N13, $x_{BA} = 0.071$). The inset of the diagram shows the absolute values of d_h at 25 and 40 °C. It is interesting to note that the hydrodynamic diameter of the collapsed microgel particles does not show a systematic change with the cross-link density, but it is practically constant. The uniformity of the collapsed particle size is probably the consequence of the identical conditions of preparation.

To get further information about the microgel particles, they were investigated by static light scattering at 25 °C. These measurements enabled the determination of the molar mass (M), the radius of gyration (R_g), and the second virial coefficient (A_2) of the microgels, as a function of their cross-link density. The results are summarized in Table 1. It is interesting to note that the very high molar mass of the "polymer" reflects that it cannot be a single chain. Further evidence for this conclusion and its structural implication will be discussed later.

Combining the experimental data measured by static and dynamic light scattering we can get structural information about the microgel particles. The ratio of the radius of gyration and the hydrodynamic radius (R_g/r_h) is a sensitive tool for monitoring the changes in the density profile of the particles. In the case of monodisperse hard spheres of constant density, this ratio is equal to 0.775. While in case of random polymer coils, it varies between 1.50 and 1.78, depending on the quality of the solvent. In Figure 3 this quantity is plotted as a function of the mole fraction of the cross-linker. In case of the large cross-link density samples (N13, N30, N50, N70) the calculated ratios are significantly smaller than that of the hard spheres. These small values (~0.6) are typical for swollen microgels and are considered as a consequence of a surface layer of the particles, where due to the decreased cross-linker concentration there is a much smaller segment density than in the core.[28,29,39] Such a loose layer can significantly increase the hydrodynamic radius of the particle but has only a small effect on the radius of gyration because of its low segment density. In Figure 3 it can also be seen that the R_g/r_h ratios exhibit a slight increase with the decrease of the mole fraction of the cross-linker (x_{BA}). This increase becomes pronounced when the cross-linker concentration decreases below $x_{BA} \approx 0.01$. The observed changes clearly indicate that the particle structure changes with the extent of cross-linking. An obvious explanation for the observed changes is that with decreasing cross-link density, the length of polymer chains dangling on the surface of the cross-linked core increases. However, the structural character of the polymer particles is determined by the ratio of the length of the dangling polymer chains to the radius of the cross-linked core, and this ratio is strongly influenced by the distribution of the cross-linker in the particles.

The average segment densities of the PNIPAM microgels can also be calculated from the light scattering data. In Figure 4 the mean polymer densities within the hydrodynamic volume of the microgel particles ($M/N_A/V_h$) are plotted at 25 and 40 °C. The mean polymer densities are approximately an order of magnitude larger in the collapsed state of the microgels (at 40 °C) than in their swollen state (at 25 °C). The determined mean-polymer densities also depend on the cross-link density of the samples. In the swollen state the mean polymer density increases strongly with the cross-link density, while in the collapsed state only a slight increase can be observed.

The mean polymer densities of the microgel particles can be used for the calculation of their water content. To make these calculations we assumed that the specific volume of the microgel particles is independent of the cross-link density, and used the specific volume values determined previously for an N13 microgel at 25 and 40 °C (0.862 and 0.877 $cm^3\ g^{-1}$, respectively).[30] These calculations show that the microgel particles contain a significant amount of water even in their collapsed state and their water content increases with the decrease of the cross-link density. In the collapsed state the water content of the microgel particles changes from ~40% to 65%, while in the swollen state the water content is in the 88−99% range.

The second virial coefficient is determined by the pair distribution function ($g(r)$) of the particles:

$$A_2 = -\frac{2\pi N_A}{M^2}\int_0^\infty [g(r) - 1]r^2\,dr \qquad (8)$$

In case of hard spheres this expression reduces to $A_{2,HS} = (N_A/M^2)4V_s$,where V_s is the volume of the hard spheres.[40] In Figure 5 the experimentally determined second virial coefficients are plotted. If we assume that the microgel particles behave like hard spheres ($r = r_h$), we can give an estimation for the second virial coefficients. The calculated values are also plotted in the

TABLE 1: Molar Mass, Radius of Gyration, and Second Virial Coefficient of the PNIPAM Microgels

	N13	N30	N50	N70	N200	N300	N400	Polym.
$M/10^8$ g mol^{-1}	3.6 ± 0.2	3.6 ± 0.1	5.2 ± 0.2	3.6 ± 0.2	2.8 ± 0.2	2.6 ± 0.1	2.5 ± 0.1	2.3 ± 0.2
R_g/nm	60 ± 11	77 ± 15	99 ± 13	93 ± 11	115 ± 12	125 ± 16	120 ± 13	159 ± 15
$A^2/10^{-6}$ mol cm^3 g^{-2}	0.59± 0.07	1.6 ± 0.1	1.5 ± 0.1	1.6 ± 0.5	2.2 ± 0.4	2.9 ± 0.4	2.0 ± 0.4	2.4 ± 0.4

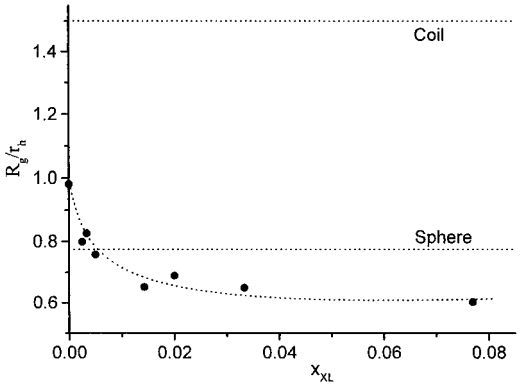

Figure 3. Cross-link density dependence of the R_g/r_h ratio of the PNIPAM microgels.

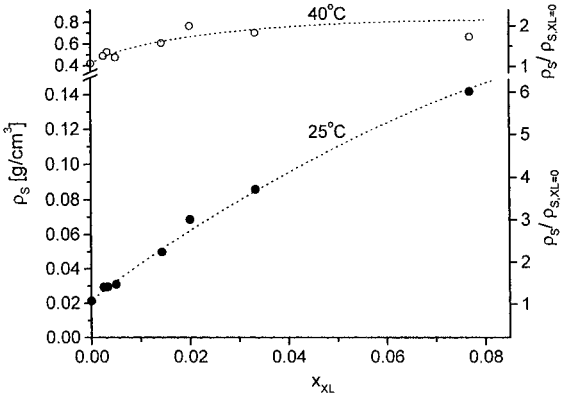

Figure 4. Cross-link density dependence of mean segment density of the PNIPAM microgels at 25 and 40 °C.

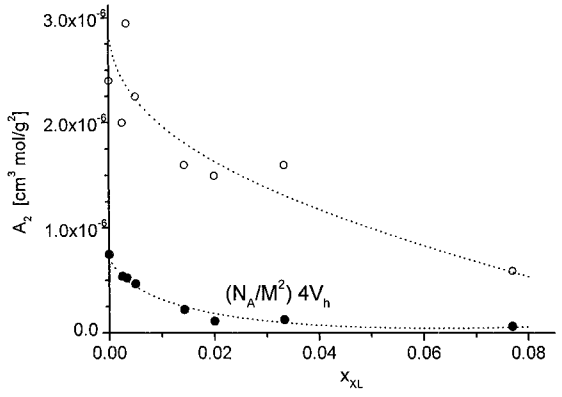

Figure 5. Measured (○) and calculated ("hard sphere", ●) second virial coefficients of the PNIPAM microgels.

figure. As can be seen, these values are much smaller than the measured ones, which means that in addition to the hard sphere like short-range interaction of the microgel particles there must be a long-range repulsive interaction between them. This repulsion can be attributed to the electrical interaction between the microgel particles that results from the presence of ionic groups originating from the initiator. This is supported by the results of light-scattering measurements done in the presence of 0.1 M NaCl for the polymer. In this case, the measured virial coefficient was (9.2 ± 2.2) × 10^{-7} mol·cm^3 g^{-2}, which is

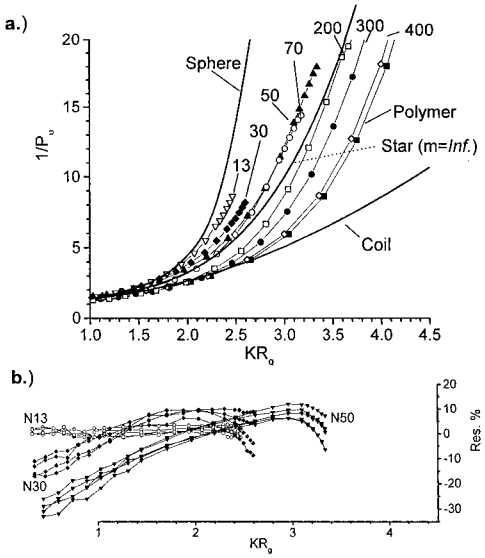

Figure 6. Experimentally determined P_ϑ^{-1} functions of the PNIPAM microgels (a). The residuals of the fitting of the experimental data with eq 7 assuming Gaussian segment density distribution in the gel particles (b).

practically equal to the value calculated from the hydrodynamic radius of the particle.

The scattered light intensity shows very strong dependence on the scattering angle in case of microgels. This angular dependence gives an opportunity for the analysis of the shape (structure) of the microgel particles on the basis of eq 7. The application of this equation is justified by the DLS measurements that indicated highly monodisperse microgel samples.

In Figure 6a the experimentally determined P_ϑ^{-1} functions are collected and plotted together with three theoretical curves (one for monodisperse spheres, another one for coils, and a third one for the asymptotic case of star polymers in which the number of arms (m) approaches infinity):

$$P_\vartheta(X) = \left[\frac{3}{X^3}\{\sin(X) - X\cos(X)\}\right]^2 \quad \left(\text{for spheres; } X = q\sqrt{\frac{20}{12}}\rho_z\right) \quad (9a)$$

$$P_\vartheta(X) = \left[\frac{2}{X^4}\{\exp(-X^2) + X^2 - 1\}\right] \quad (\text{for coils; } X = q\rho_z) \quad (9b)$$

$$P_\vartheta(X) = 2\left(1 - \frac{1}{m}\right)P_{\vartheta,2}(X) - \left(1 - \frac{2}{m}\right)P_{\vartheta,1}(X) \quad (\text{for stars; } X = q\rho_z) \quad (9c)$$

where $P_{\vartheta,2}(X)$ and $P_{\vartheta,1}(X)$ are the P_ϑ functions of coils built up by two arms and one arm of the star, respectively. Based on the figure we can make the following statements:

The measured P_ϑ^{-1} functions can be found between the P_ϑ^{-1} functions of spheres and coils.

Though the microgel particles are considered in the literature as homogeneous spheres independently of their cross-link

density, even the P_ϑ^{-1} function of the most cross-linked microgel (N13) shows significant deviations from that of a homogeneous sphere.

With decreasing cross-link density, the P_ϑ^{-1} functions change systematically toward the P_ϑ^{-1} function of coils.

The P_ϑ^{-1} functions of the less cross-linked microgels fall in a region where the P_ϑ^{-1} functions of the star polymers can also be found (between that of a coil, one arm stars, and the asymptotic P_ϑ^{-1} function of stars with $m = \infty$ arms). It is interesting to note that in case of these microgels the R_g/r_h ratios are larger than the value characteristic for the microgels.

Taking into account that according to electron micrographs the microgel particles have spherical symmetry, in principle there are two factors that can have the observed effect on the P_ϑ^{-1} functions of the microgels. On one hand, the microgel particles can have a cross-linked core that is surrounded by a shell of dangling polymer chains. On the other hand, the radial segment density distribution of the cross-linked particle core is not necessarily constant.

In the case of large cross-link densities, it seems to be a reasonable assumption that the size of the dangling chains is negligible compared to the particle size, so the microgels retain their particle character. To check the validity of this assumption we tried to fit the experimental data with eq 7 using the P_ϑ function of particles having a spherical density distribution:[41]

$$P_\vartheta = \frac{1}{V^2}[\int F(\xi)\cos(K\xi)\,d\xi]^2 \qquad (10)$$

where ξ is the distance from the center of a particle to a plane that has a constant phase shift referred to this center and

$$F(\xi) = 2\pi\int_{A(\xi)}\rho\,\alpha(\xi,\rho)\,d\rho$$

in which α is the radial segment density distribution of the particle, and $A(\xi)$ is a constant-phase plane that is at a distance ξ from the center of the particle. The exact form of this function is determined by the radial-segment density distribution and generally can be calculated numerically. Though we tried to fit the experimental data with several different segment density distributions, we could get reasonable fits only for the most cross-linked microgel (N13) assuming a Gaussian segment density distribution. (The residuals of a few fits can be seen in Figure 6b.) Since it can be expected that the local cross-link density changes similarly as the local-segment density of the swollen particle, the observed Gaussian-segment density distribution implies that the cross-link density decreases from the center of the particle toward its periphery, which is in agreement with the results of kinetic measurements.[25,26]

It is important to note that the light-scattering data can be interpreted by considering the microgels as particles having a nonuniform-segment density distribution only in case of the most cross-linked microgel (N13). This indicates that even a microgel having as large average cross-link density as the N30, has already lost its "well-defined" gel particle character and it starts exhibiting coillike behavior. This can be interpreted as a consequence of the accumulation of the cross-linker in the core of the particles. Moving away from the center of the particle, the initial cross-link density rapidly decreases leaving a shell of dangling polymer chains connected to the cross-linked core.

The P_ϑ^{-1} function of the PNIPAM sample prepared without cross-linker (polymer in Figure 6) significantly differs from that of a single polymer chain. However, it is known that during emulsion polymerization the radical/monomer ratio can be as high as 1:1 in the monomer swollen polymer particle, which results in significant chain branching. The observed P_ϑ^{-1} function of the "polymer" clearly reflects the effect of such a chain branching reaction.

With the addition of the cross-linking monomer to the reaction mixture at the beginning of the reaction, the radical/monomer (unreacted double bond) ratio decreases significantly, since a considerable fraction of the monomers incorporated in the polymer chains contains an additional double bond. This means that instead of the chain branching reaction, primarily the much more favorable cross-linking reaction will take place. On the other hand, at the end of the reaction, when the concentration of the cross-linking monomer becomes sufficiently small, branching can become effective, resulting in the formation of a compact, non-crosslinked outer shell of the particles.

With increasing the amount of cross-linker added to the reaction mixture, the size of a strongly cross-linked core increases and the structure of the microgel particles gradually tends from a highly branched polymer toward a compact gel particle possessing a nonuniform segment density distribution.

Acknowledgment. This work was supported by the Hungarian Scientific Research Fund (No. T029780).

References and Notes

(1) Gandhi, M. V.; Thompson, B. S. *Smart materials and structures;* Chapman & Hall: London, 1992.
(2) *Polyelectrolyte Gels: Properties, Preparation, and Applications*, Harland, R. S., Prud'homme, R. K., Eds.; ACS Symposium Series 480; American Chemical Society: Washington, DC, 1992.
(3) Osada, Y. *Adv. Polym. Sci.* **1987**, *82*, 1.
(4) Bradna, P.; Stern, P.; Quadrat, O.; Snuparek, J. *Colloid Polym. Sci.* **1995**, *273*, 324.
(5) Murry, M. J.; Snowden, M. J. *Adv. Coll. Interface Sci.* **1995**, *54*, 73.
(6) Morris, G. E.; Vincent, B.; Snowden, M. J. *J. Colloid Interface Sci.* **1997**, *190*, 1980.
(7) *Polymer Gels: Fundamentals and Biomedical Applications*; DeRossi, D.; Kajiwara, K.; Osada, Y.; Yamauchi, A., Eds.; Plenum Press: New York, 1991.
(8) Antonietti, M. *Angew. Chem.* **1988**, *100*, 1813.
(9) Bartsch, E. *Transp. Theor. Stat. Phys.* **1995**, *24*, 1125.
(10) Bartsch, E.; Frenz, V.; Baschnagel, J.; Schärtl, W.; Sillescu, H. *J. Chem. Phys.* **1997**, *106*, 3743.
(11) Wu, C.; Zhou S. *Macromolecules* **1996**, *29*, 1574.
(12) Pelton, R.; Wu, X.; McPhee, W.; Tam, C. In *Colloidal Polymer Particles*, Goodwin, J. W., Buscall, R. Eds.; Academic: London, 1995.
(13) Wu, C.; Zhou, S. *Macromolecules* **1995**, *28*, 8381.
(14) Walter, R.; Ricka, J.; Quellet, Ch.; Nyffenegger, R.; Binkert, Th. *Macromolecules* **1996**, *29*, 4019.
(15) Kratz, K.; Eimer, W. *Ber. Bunsen-Ges. Phys. Chem.* **1998**, *102*, 848.
(16) Kratz, K.; Hellweg, T.; Eimer, W. *Ber. Bunsen-Ges. Phys. Chem.* **1998**, *102*, 1603.
(17) Shibayama, M.; Muzutani, S. Y.; Nomura, S. *Macromolecules* **1996**, *29*, 2019.
(18) Saunders, B. R.; Vincent, B. *Adv. Colloid Interface Sci.* **1999**, *80*, 1.
(19) Crowther, H. M.; Saunders, B. R.; Mears, S. J.; Cosgrove, T.; Vincent, B.; King, S. M.; Yu, G. *Colloids Surf.* **1999**, *152*, 327.
(20) Saunders, B. R.; Crowther, H. M.; Vincent, B. *Macromolecules* **1997**, *30*, 482.
(21) Saunders, B. R.; Vincent, B. *J. Chem. Soc., Faraday Trans.* **1996**, *92*, 3385.
(22) Crowther, H. M.; Vincent, B. *Colloid Polym. Sci.* **1998**, *276*, 46.
(23) Tanaka, T.; Fillmore, D. J. *J. Chem. Phys.* **1979**, *70*, 1214.
(24) Mears, S. J.; Deng, Y.; Cosgrove, T.; Pelton, R. *Langmuir* **1997**, *13*, 1901.
(25) McPhee, W.; Tam, K. C.; Pelton, R. *J. Colloid Interface Sci.* **1993**, *24*, 156.
(26) Schild, H. G. *Prog. Polym. Sci.* **1992**, *17*, 163.
(27) Bartsch, E.; Kirsch, S.; Lindner, P.; Scherer, T.; Stolken, S. *Ber. Bunsen-Ges. Phys. Chem.* **1998**, *102*, 1597.
(28) Senff, H.; Richtering, W. *J. Chem. Phys.* **1999**, *111*, 1705.
(29) Senff, H.; Richtering, W. *Colloid Polym. Sci.* **2000**, *278*, 821.

(30) Gilányi, T.; Varga, I.; Mészáros, R.; Filipcsei, G.; Zrínyi, M. *Phys. Chem. Chem. Phys.* **2000**, *2*, 1973.

(31) Wu, X.; Pelton, R. H.; Hamielec, A. E.; Woods, D. R.; McPhee, W. *Colloid Polym. Sci.* **1994**, *272*, 467.

(32) Vanderhoff, J. W. *Pure Appl. Chem.* **1980**, *52*, 1263.

(33) Gardiner, C. W. *Handbook of Stochastic Methods;* Springer: Berlin, 1990.

(34) King, T. A.; Treadaway, M. F. *J. Chem. Soc., Faraday Trans. 2*, **1977**, *73*, 1616.

(35) Berne, B. J.; Pecora, R. *Dynamic Light Scattering;* Wiley & Sons: New York, 1976.

(36) Schmitz, K. S. An Introduction to Dynamic Light Scattering by Macromolecules; Academic Press: Boston, 1990.

(37) Chu, B. *Laser Light Scattering;* Academic Press: Boston, 1991.

(38) Inomata, H.; Wada, N.; Yagi, Y.; Goto, S.; Saito, S. *Polymer* **1995**, *36*, 875.

(39) Schmidt, M.; Nerger, D.; Burchard, W. *Polymer* **1979**, *20*, 582.

(40) Higgins, J. S.; Benoit, H. C. *Polymers and Neutron Scattering*, Oxford University Press: Oxford, 1994.

(41) Bohren, F. C.; Huffman, D. R. *Absorption and Scattering of Light by Small Particles;* Wiley & Sons: New York, 1983.